

# The implications of bias correction methods and climate model ensembles on soil erosion projections under climate change

Joris P. C. Eekhout\* and Joris de Vente

Soil and Water Conservation Research Group, CEBAS-CSIC, Spanish Research Council, Murcia, Spain

Received 3 August 2018; Revised 13 November 2018; Accepted 4 December 2018

\*Correspondence to: Joris P. C. Eekhout, Soil and Water Conservation Research Group, CEBAS-CSIC, Spanish Research Council, Campus Universitario Espinardo, 30100, PO Box 164, Murcia, Spain. E-mail: joriseekhout@gmail.com



**ABSTRACT:** Climate change will most likely cause an increase in extreme precipitation and consequently an increase in soil erosion in many locations worldwide. In most cases, climate model output is used to assess the impact of climate change on soil erosion; however, there is little knowledge of the implications of bias correction methods and climate model ensembles on projected soil erosion rates. Using a soil erosion model, we evaluated the implications of three bias correction methods (delta change, quantile mapping and scaled distribution mapping) and climate model selection on regional soil erosion projections in two contrasting Mediterranean catchments. Depending on the bias correction method, soil erosion is projected to decrease or increase. Scaled distribution mapping best projects the changes in extreme precipitation. While an increase in extreme precipitation does not always result in increased soil loss, it is an important soil erosion indicator. We suggest first establishing the deviation of the bias-corrected climate signal with respect to the raw climate signal, in particular for extreme precipitation. Furthermore, individual climate models may project opposite changes with respect to the ensemble average; hence climate model ensembles are essential in soil erosion impact assessments to account for climate model uncertainty. We conclude that the impact of climate change on soil erosion can only accurately be assessed with a bias correction method that best reproduces the projected climate change signal, in combination with a representative ensemble of climate models. © 2018 John Wiley & Sons, Ltd.

**KEYWORDS:** bias correction; soil erosion; climate change; impact assessment; extreme precipitation

## Introduction

Climate change will most likely cause an increase in extreme precipitation in many locations worldwide (Sun *et al.*, 2007), which will impact hydrological and geomorphological processes, such as an increase in flooding (Blöschl *et al.*, 2015), landslides (Crozier, 2010) and soil erosion (Nearing *et al.*, 2004). The impact of climate change on soil erosion and sediment yield is assessed by applying soil erosion models, which are commonly forced by model output from an ensemble of global climate models (GCMs). Owing to the coarse GCM grid and the bias between local observations and the historical GCM model output, GCM output requires correction before being applied in model assessments. Here we focus on the correction applied to precipitation data from climate models, most relevant for soil erosion assessments.

Downscaling is used to transform the coarse spatial scale of the GCM output to the spatial scale most appropriate for model assessments and can be classified into two groups: dynamical and statistical downscaling (Boé *et al.*, 2007). Dynamical downscaling involves the application of higher resolution (<50 km) regional climate models (RCMs), which often have a continental-scale spatial domain. The boundary conditions of an RCM originate from the original GCM and are

thus nested within the coarse GCM grid. Statistical downscaling involves the establishment of an empirical relation between larger-scale climate and local-scale variables, such as land-use, topography and land-sea contrast. Comparison studies have shown that dynamical and statistical downscaling often lead to similar results (e.g. Maraun *et al.*, 2010; Hertig *et al.*, 2012; Vaittinada Ayar *et al.*, 2016; Le Roux *et al.*, 2018). The main disadvantage of dynamic downscaling is that it is computationally demanding. However, the Coordinated Regional Downscaling Experiment (CORDEX; Giorgi *et al.*, 2009) provides an internationally coordinated framework from which a large number of freely available RCM output can be downloaded for various spatial domains.

Commonly, climate models (both GCM and RCM) produce a bias between the historical model output and observations, which can be corrected by applying bias correction methods (Teutschbein and Seibert, 2012). The delta change method (Déqué, 2007) is the most widely used bias correction method in soil erosion assessments (supporting information, Figure S1 and Table S1). This method is most often applied at a low temporal resolution, i.e. annual or monthly. Consequently, higher temporal climate signals, such as extreme precipitation, are lost. This can be overcome by applying more advanced bias correction methods, such as quantile mapping

(Wood *et al.*, 2004). Quantile mapping is based on the empirical cumulative density distribution function (ECDF) of the precipitation time series. Hereby, this method is able to preserve projected changes in precipitation intensity and frequency. However, quantile mapping also assumes that the ECDF of the observations can be applied to the projected time series (stationarity assumption; Themeßl *et al.*, 2012), which is responsible for altering (often overestimating) the raw model projections (Maurer and Pierce, 2014). To resolve some of the inaccuracy of the quantile mapping method several alternative methods have been proposed recently, such as detrended quantile mapping (Hempel *et al.*, 2013), quantile delta mapping (Cannon *et al.*, 2015) and scaled distribution mapping (Switanek *et al.*, 2017).

Climate models (both GCMs and RCMs) provide a range of climate projections, due to the variety of numerical formulations and physical parametrization schemes (Chen *et al.*, 2017). As a result, climate model output is a source of uncertainty in climate change impact studies in addition to other sources, such as impact models, emission scenarios, and bias correction and downscaling methods (Chen *et al.*, 2017). Climate model uncertainty is found to be one of the dominant sources of uncertainty (Chen *et al.*, 2011b); hence many studies apply a climate model ensemble to account for the uncertainty among the different climate models (Teutschbein and Seibert, 2010). However, many climate change assessments on soil erosion apply only one climate model (supporting information, Figure S2 and Table S1) and, therefore, most likely do not sufficiently account for climate model uncertainty.

Some authors have acknowledged that downscaling and bias correction of climate projections is one of the key weaknesses of previous climate change assessments on soil erosion (Mullan *et al.*, 2012; Li and Fang, 2016). The first assessments were performed at the beginning of the 1990s and applied hypothetical scenarios of changes in annual precipitation (Boardman *et al.*, 1990; Favis-Mortlock *et al.*, 1991). Rainfall intensity is one of the main drivers for soil erosion (Boardman and Favis-Mortlock, 1993; Nearing *et al.*, 2004). Moreover, an increase in rainfall intensity is likely to be one of the most dominant threats to soil erosion (Boardman and Favis-Mortlock, 1993; Nearing *et al.*, 2004). Furthermore, soil erosion is found to be more sensitive to changes in rainfall intensity than to changes in precipitation sum (Pruski and Nearing, 2002b; Nunes *et al.*, 2009). Obviously, the delta change method is not able to fully account for the changes in rainfall intensity, and studies that apply the delta change method often show that a change in annual rainfall leads to a similar direction of change in soil erosion (e.g., Shrestha *et al.*, 2013; Correa *et al.*, 2016). For climate change impact assessments, one of the most essential considerations is the use of downscaling and bias correction methods that account for changes in the precipitation distribution. Statistical downscaling methods and quantile mapping have proven to be able to transfer projected increase in rainfall intensity from GCM output to soil erosion model input, reflected in an increase in soil erosion (e.g. Mullan *et al.*, 2012; Routschek *et al.*, 2014; Lacoste *et al.*, 2015; Paroissien *et al.*, 2015; Kourgialas *et al.*, 2016).

The most applied bias correction methods in soil erosion assessments either insufficiently account for changes in the precipitation distribution (delta change) or may lead to an overestimation of rainfall intensity (quantile mapping) (Mullan *et al.*, 2012; Maurer and Pierce, 2014; Li and Fang, 2016). In this study, we compared these two bias correction methods and a recent alternative called scaled distribution mapping, and assessed the implications of applying bias correction in climate change assessments on soil erosion. Furthermore, we

applied a climate model ensemble to account for the uncertainty in climate model output and to assess the impact of individual climate models on soil erosion. The three bias correction methods and the climate model ensemble were evaluated in two contrasting Mediterranean catchments, using the SPHY-MMF soil erosion model (Ekhout *et al.*, 2018b).

## Material and Methods

### Study area

This study was performed in two similar-sized subcatchments of the Segura river basin in southeastern Spain (Figure 1 and Table I). The two catchments mainly differ in climate and land use. The Sierra de Segura catchment is predominantly classified as Mediterranean climate (temperate, dry summer), where the annual precipitation sum equals 544 mm (1981–2000; Serrano-Notivoli *et al.*, 2017). The Guadalentin is predominantly classified as semi-arid, with an annual precipitation sum of 295 mm (1981–2000; Serrano-Notivoli *et al.*, 2017). The Sierra de Segura catchment is dominated by natural land use (forest, 45.0%; shrubland, 39.6%). The Guadalentin catchment has mixed land use, with shrubland (30.7%), forest (22.7%), cereals (17.5%) and tree crops (16.9%) as the most dominant land-use classes. Hence the Guadalentin catchment can be considered an agricultural catchment, with a total cover of 43.3%. The most dominant soil texture classes are Leptosols (37.8%) and Luvisols (26.6%) in the Sierra de Segura catchment, and Calcisols (45.5%) and Leptosols (72%) in the Guadalentin catchment. The elevation ranges between 411 and 2055 m above sea level and the slope averages 16.3% in the Sierra de Segura catchment. The elevation ranges between 211 and 2034 m above sea level and the slope averages 9.2% in the Guadalentin catchment.

### Climate data

We applied one emission scenario (Representative Concentration Pathway; RCP8.5) divided over two future periods, i.e. 2031–2050 and 2081–2100, denoted as the foreseeable-future and the far-future scenarios, respectively. RCP8.5 represents a high-emission scenario with a continuous increase in emissions throughout the 21st century. We obtained data from a total of nine climate models (GCM/RCM combinations; Table II) from the EURO-CORDEX initiative (Jacob *et al.*, 2014), with a 0.11° resolution. Precipitation data for the reference period (1981–2000) were obtained from the SPREAD daily dataset (Serrano-Notivoli *et al.*, 2017), with a 5 km resolution. Temperature data for the reference period were obtained from the SPAIN02 daily dataset (Herrera *et al.*, 2016), with a 0.11° resolution.

### Bias correction methods

The raw climate data were bias corrected using monthly delta change (DC), quantile mapping (QM) and scaled distribution mapping (SDM). All methods are applied for each grid cell separately. In the description of the three methods we focus on the bias correction of precipitation data only, which is most relevant for this study. We also applied bias correction to the temperature datasets, which are used as input for the hydrological model. For details regarding bias correction of the temperature data, we refer to Chen *et al.* (2011a; DC), Themeßl *et al.* (2012; QM) and Switanek *et al.* (2017; SDM).

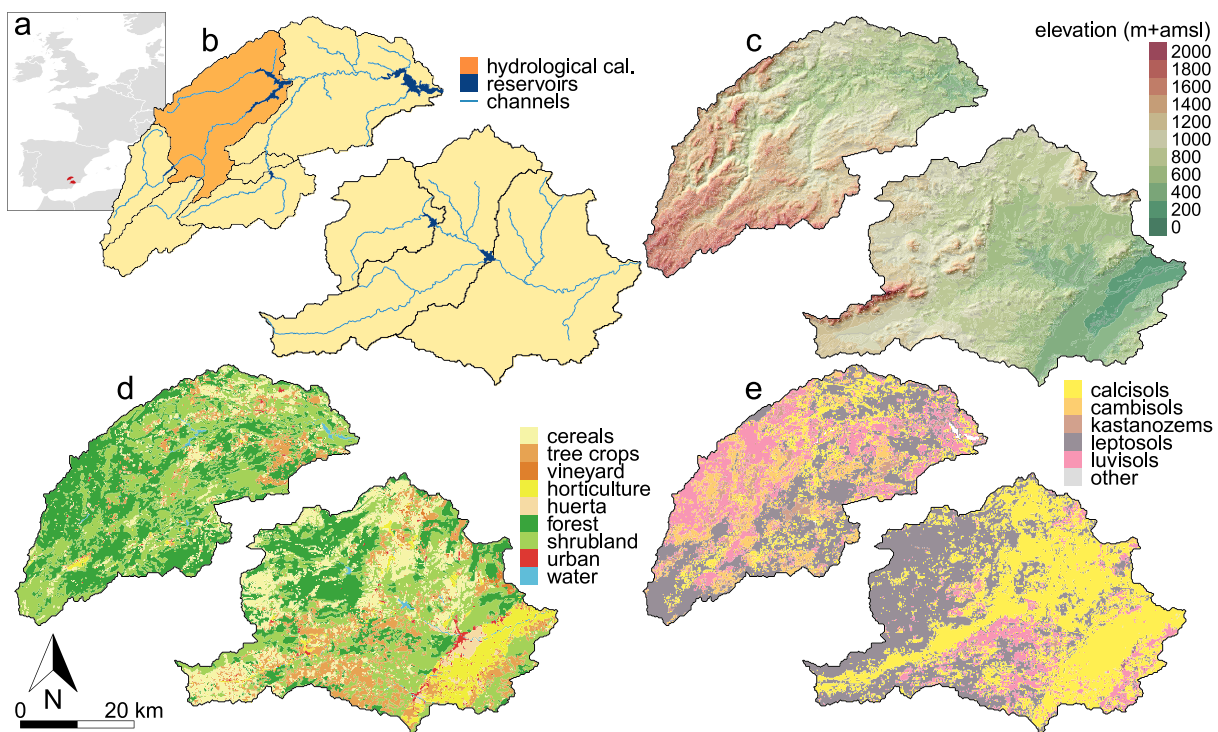


**Figure 1.** Location and characteristics of the Sierra de Segura and Guadalentin catchments: (a) location of the two catchments within Europe; (b) hydrological calibration area (orange), channels (light blue) and reservoirs (dark blue); (c) digital elevation model (Farr *et al.*, 2007); (d) land-use map (MAPAMA, 2010); (e) soil texture map (Hengl *et al.* 2017)

**Table I.** Characteristics of the two catchments

	Unit	Sierra de Segura	Guadalentin
Area	km <sup>2</sup>	2589.04	2628.68
Annual precipitation sum	mm	544.4	294.9
Average temperature	°C	13.24	14.73
Dominant climate classification (Köppen)		Cs (67.2%)	BS (86.9%)
Cereals	%	7	17.5
Tree crops	%	6.4	16.8
Vineyard	%	0.2	0.9
Horticulture	%	0.4	8.1
Huerta	%	0.6	1.5
Forest	%	45.0	22.7
Shrubland	%	39.6	30.7
Urban	%	0.3	1.2
Water	%	0.5	0.6

**Table II.** The nine climate models used in this study, with their corresponding RCM, GCM and research institute

GCM	RCM				
	CCLM <sup>a</sup>	HIRHAM5 <sup>b</sup>	RACMO <sup>c</sup>	RCA <sup>d</sup>	WRF <sup>e</sup>
CNRM-CM5	×				×
EC-EARTH	×	×	×	×	×
IPSL-CM5A-MR					×
MPI-ESM-LR	×			×	

<sup>a</sup> Climate Limited-area Modelling Community (CLMcom).

<sup>b</sup> Danish Meteorological Institute (DMI).

<sup>c</sup> Royal Netherlands Meteorological Institute (KNMI).

<sup>d</sup> Swedish Meteorological and Hydrological Institute (SMHI).

<sup>e</sup> Institut Pierre Simon Laplace (IPSL).

### Delta change

We applied the DC method as proposed by Chen *et al.* (2011a). To obtain the bias-corrected projection of future daily precipitation ( $P_{\text{mod,fut,BC}}$ ), we multiplied the observed daily precipitation for the reference period ( $P_{\text{obs,ref}}$ ) by the monthly-averaged precipitation ratio between the raw climate model output for the future period ( $\bar{P}_{\text{mod,fut}}$ ) and the reference period ( $\bar{P}_{\text{mod,ref}}$ ):

$$P_{\text{mod,fut,BC}} = P_{\text{obs,ref}} \times \left( \frac{\bar{P}_{\text{mod,fut}}}{\bar{P}_{\text{mod,ref}}} \right) \quad (1)$$

### Quantile mapping

We applied the QM method as proposed by Themeßl *et al.* (2012). QM is applied on a daily basis. First the empirical cumulative density distribution function is determined for the observations in the reference period ( $\text{ECDF}_{\text{obs,ref}}$ ) and for the climate model output in the reference period ( $\text{ECDF}_{\text{mod,ref}}$ ). The ECDFs are determined for each day of the year (doy), centred within a 31-day moving window. The probability (Prob) is then determined for the occurrence of precipitation on a particular day in the future  $P_{\text{mod,fut}}$  to the corresponding ECDF in the reference period:

$$\text{Prob} = \text{ECDF}_{\text{mod,ref}}(P_{\text{mod,fut}}) \quad (2)$$

A correction factor CF is determined by feeding probability Prob in the inverse ECDFs for both the observed and model output:

$$\text{CF} = \text{ECDF}_{\text{obs,ref}}^{-1}(\text{Prob}) - \text{ECDF}_{\text{mod,ref}}^{-1}(\text{Prob}) \quad (3)$$

Finally, CF is added to the raw future climate model output to obtain the bias-corrected value:

$$P_{\text{mod,fut,BC}} = P_{\text{mod,fut}} + \text{CF} \quad (4)$$

We adopted the QM method proposed by Themeßl *et al.* (2012), which accounts for uncertainties when the dry-day frequency of the historical climate model output is greater than in the historical observations (dry-day frequency). Furthermore, this method corrects for future extreme precipitation values that do not occur in the historical observations (new extremes).

#### Scaled distribution mapping

We applied the novel SDM method (Switanek *et al.*, 2017), which does not make the assumption of stationarity. This method scales the observed precipitation distribution by raw-model projected changes in magnitude, rain-day frequency and likelihood of events. SDM consists of seven steps as outlined below. All calculations are performed for each month separately. We refer to the observed, modelled historical and modelled projected data as the three precipitation datasets.

1. The expected number of rain days for the bias-corrected future period ( $RD_{BC}$ ) is determined, based on number of rain days from the three precipitation datasets:

$$RD_{BC} = RD_{mod,fut} \times \frac{RD_{obs,ref}/TD_{obs,ref}}{RD_{mod,ref}/TD_{mod,ref}} \quad (5)$$

where  $RD_{mod,fut}$ ,  $RD_{obs,ref}$  and  $RD_{mod,ref}$  are the number of rain days of the future model, observations and historical model, and  $TD_{obs,ref}$  and  $TD_{mod,ref}$  are the total number of days of the observations and historical model. The number of rain days is determined with a minimum precipitation threshold, which is set to 0.1 mm, following Switanek *et al.* (2017).

2. A gamma distribution is fitted to the three precipitation datasets, and the shape and scale parameters are determined using maximum likelihood. Based on these two parameters, the cumulative distribution function (CDF) is determined for each of the three precipitation datasets, with an upper threshold of 0.999999.
3. A scaling factor ( $SF_R$ ) is determined between the fitted future model distribution and the fitted historical model distribution at the CDF values corresponding to the precipitation events of the future model time series:

$$SF_R = \frac{ICDF_{mod,fut}(CDF_{mod,fut})}{ICDF_{mod,ref}(CDF_{mod,ref})} \quad (6)$$

where  $ICDF_{mod,fut}$  and  $ICDF_{mod,ref}$  are the inverse CDFs of the fitted future model and fitted historical model distributions, and  $CDF_{mod,fut}$  the estimated CDF values of the future model from the previous step.

4. The recurrence interval (RI) of each of the three sorted precipitation datasets is determined:

$$RI = \frac{1}{1 - CDF} \quad (7)$$

where CDF is obtained from step 2. The recurrence intervals of the observed and modelled historical precipitation datasets are linearly interpolated to the length of the future modelled data.

5. The scaled recurrence interval ( $RI_{SCALED}$ ) is determined based on the (interpolated) recurrence intervals of the previous step:

$$RI_{SCALED} = \max \left( 1, \frac{RI_{obs,ref} \times RI_{mod,fut}}{RI_{mod,ref}} \right) \quad (8)$$

The CDF of the scaled recurrence interval ( $CDF_{SCALED}$ ) is determined and subsequently sorted in descending order:

$$CDF_{SCALED} = 1 - \frac{1}{RT_{SCALED}} \quad (9)$$

The CDF of the scaled recurrence interval reflects the scaling of the modelled change (future vs. historical) in event likelihood with respect to the observed likelihoods.

6. An initial array of bias-corrected values is obtained with input from the previous steps, i.e. the inverse CDF of the observations ( $ICDF_{mod,ref}$ ; step 2), the scaled CDF ( $CDF_{SCALED}$ ; step 5) and the scaling factor ( $SF_R$ ; step 3):

$$BC_{INITIAL} = ICDF_{obs,ref}(CDF_{SCALED}) \times SF_R \quad (10)$$

7. Finally, the array of bias-corrected values are placed back in the correct temporal locations of the future modelled time series, i.e. the highest bias-corrected value is reinserted to the day with the highest projected rainfall; the second highest bias-corrected value is reinserted to the day with second highest projected rainfall; and so on.

#### Hydrological and soil erosion model

We applied the SPHY-MMF model (Eekhout *et al.*, 2018b), a spatially distributed hydrological model, fully coupled with a soil erosion model. The model is applied on a cell-by-cell basis, with a fixed resolution of 200 m and a daily time step. The Spatial Processes in HYdrology model (SPHY; Terink *et al.*, 2015) simulates most relevant hydrological processes, i.e. interception, evapotranspiration, surface runoff, and lateral and vertical soil moisture flow. The Morgan–Morgan–Finney model (MMF; Morgan and Duzant, 2008) simulates most relevant soil erosion processes, such as soil detachment by raindrop impact and runoff, sediment deposition and sediment routing. The model also includes a vegetation model. Based on the spatial and temporal variation of the Normalized Differentiated Vegetation Index (NDVI), the vegetation model determines actual evapotranspiration (crop coefficient established from NDVI), interception, canopy storage, throughfall and canopy cover. No NDVI images were available for the reference and the future periods; therefore, we determined NDVI based on a land-use-specific log-linear relationship between NDVI and climate conditions (precipitation and temperature) obtained from a calibration period (2000–2012) (see Eekhout *et al.*, 2018a, for details). The observed and bias-corrected precipitation and temperature data were interpolated on the model grid using bivariate interpolation (Akima, 1996).

The hydrological model was calibrated in the Fuensanta subcatchment, located in the Sierra de Segura catchment (Figure 1b) for the period 2001–2010 and validated for the period 1987–2000 using daily observed discharge data. Intense rainfall events have most impact on soil erosion (Nearing *et al.*, 1990). Therefore, in the calibration procedure, we focused on the large discharge events. We used a baseflow separation algorithm to separate large discharge events from the rest of the time series using the method proposed by Ladson *et al.* (2013). We used a threshold of twice the calculated baseflow to separate the discharge events, which occurs 19% of the time. We applied the Statistical Parameter Optimization Tool PYthon package (SPOTPY; Houska *et al.*, 2015) to calibrate the hydrological model, using the Simulated Annealing algorithm and the Nash–Sutcliffe model efficiency (NSE; Nash and Sutcliffe, 1970). The calibration on daily discharge data resulted in an NSE of 0.61 and the validation in an NSE of 0.35 (Figure 2).

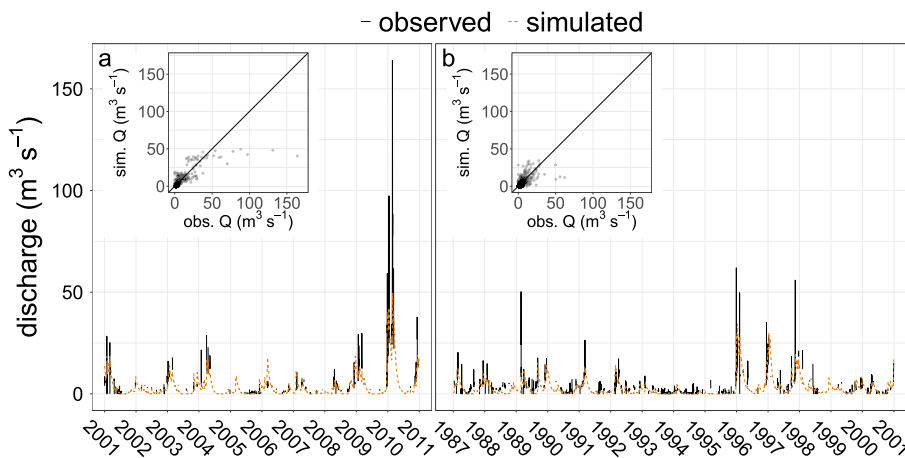


**Figure 2.** Discharge time series for the calibration (a) and validation period (b). The solid black line correspond to the observed time series and the dashed orange line corresponds to the simulated time series

**Table III.** Calibration and validation of annual unit soil loss and comparison with literature data ( $\text{Mg km}^{-2} \text{yr}^{-1}$ )

Land-use class	Calibration	Validation	Maetens <i>et al.</i> (2012)
Cereals	234.8	143.4	230.0
Tree crops	297.4	231.9	300.0
Vineyard <sup>a</sup>	298.5	267.1	300.0
Horticulture	234.7	204.8	230.0
Huerta	238.2	253.5	230.0
Forest <sup>b</sup>	41.6	34.0	40.0
Shrubland	32.1	26.3	30.0
Urban/water	0.0	0.0	n.a.

<sup>a</sup> Annual unit soil loss not available; value of tree crops used instead.

<sup>b</sup> annual unit soil loss not available; annual soil loss used instead.

The soil erosion model was calibrated for the period 2001–2010 and validated for the period 1981–2000 using observed plot-scale literature data (Maetens *et al.*, 2012). The model was calibrated with annual unit soil loss ( $SL_u$ ) using the method described by Maetens *et al.* (2012), which is soil loss corrected for plot length and slope gradient. We obtained data that correspond to the Mediterranean region (Maetens *et al.*, 2012, table 7). To allow comparison with measured hillslope erosion, we only used the cells with a contributing area smaller than  $2 \text{ km}^2$ . This threshold was established because cells with a larger contributing area tend to overestimate soil loss on hillslopes (Eekhout *et al.*, 2018b). The soil loss obtained from the model was averaged per land-use class (see Table III for calibration and validation results).

## Uncertainty analysis

We applied a total of 12 scenarios, representing two future periods, two catchments and three bias correction methods. In each scenario, we applied an ensemble of nine climate models; hence we performed 108 model simulations. To account for uncertainty we evaluated the significance of the climate projections and the model predictions within the ensemble of nine climate models. A paired U-test (Mann–Whitney–Wilcoxon test, with a significance level of 0.05) was applied to test the significance of model outcomes for the nine climate models. The pairs consisted of the model output for (1) the reference scenario and (2) the nine climate models. The paired U-test was also applied to determine the

significance of the catchment-averaged change with respect to the reference scenario.

## Results

All three bias correction methods project a decrease in annual precipitation sum (Figure 3 and Table IV). In the foreseeable-future scenario, a significant decrease is projected in large parts of the Sierra de Segura catchment, whereas the Guadalentin catchment shows mainly non-significant changes in annual precipitation sum. In the far-future scenario, all three bias correction methods project a significant decrease in annual precipitation sum in both catchments. Most decrease is projected in the Sierra de Segura catchment, up to a catchment average of 147 mm ( $-27.0\%$ ) with the SDM method.

The impact of climate change on extreme precipitation may be a more relevant indicator for soil erosion assessments than annual precipitation, and demonstrates the most important difference between the three bias correction methods. Here, we quantified extreme precipitation following the definition by Jacob *et al.* (2014), which defines extreme precipitation as the 95th percentile of daily precipitation, considering only rainy days ( $>1 \text{ mm d}^{-1}$ ). In the foreseeable-future scenario the DC method projects a significant decrease in extreme precipitation in the Sierra de Segura catchment, whereas in the Guadalentin catchment an increase is projected (n.s.) (Figure 4). In the far-future scenario, the DC method projects a significant decrease in extreme precipitation in both catchments. The QM method projects a significant increase in extreme precipitation in both catchments and periods. The SDM method projects a non-significant increase in both catchments and periods.

In the reference scenario most soil loss is projected in the Guadalentin catchment, mainly due to the higher extent of arable land compared to the Sierra de Segura catchment (Figure 5 and Table V). In the foreseeable-future scenario, the DC method projects a decrease in the Sierra de Segura catchment (n.s.) and an increase in the Guadalentin catchment (n.s.). In the far-future scenario, the DC method projects a significant decrease in soil loss in the Sierra de Segura catchment. In the Guadalentin catchment, a catchment-average decrease is projected (n.s.), while spatially a heterogeneous response is projected (increase and decrease). The QM and SDM methods project an increase in soil loss in the foreseeable-future scenario, with significant increases for the Guadalentin catchment. In the far-future scenario, the QM and SDM methods

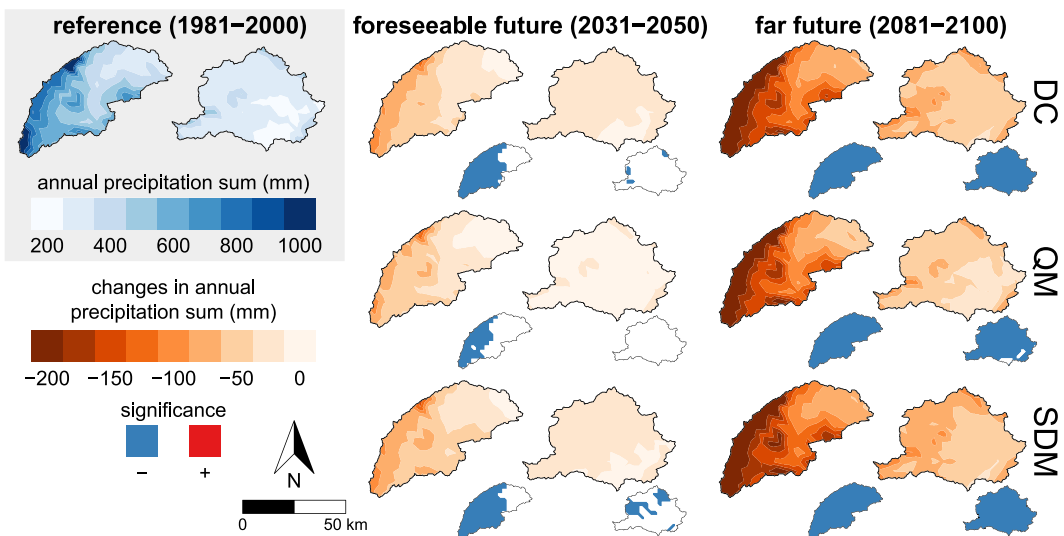


**Figure 3.** Ensemble average annual precipitation sum (mm) for the reference scenario (1981–2000; left) and changes between the reference scenario and the two future scenarios (2031–2050, middle; 2081–2100, right) for each bias correction method. The small maps in the right bottom corner of each map represent significance, where blue indicates a significant decrease and red a significant increase ( $p < 0.05$ )

**Table IV.** Catchment-average annual precipitation sum (mm), extreme precipitation (mm) and average temperature ( $^{\circ}$ C) from the reference scenario, and difference between the reference and future scenarios, accompanied by percentages in parentheses

	Sierra de Segura (2031–2050)	Guadalentin (2031–2050)	Sierra de Segura (2081–2100)	Guadalentin (2081–2100)
<i>Annual precipitation sum (mm)</i>				
Ref.	544.4	294.9	544.4	294.9
DC	<b>-44.0 (-8.1)</b>	-17.1 (-5.8)	<b>-139.1 (-25.5)</b>	<b>-59.5 (-20.2)</b>
QM	-36.5 (-6.7)	-6.1 (-2.1)	<b>-134.5 (-24.7)</b>	<b>-45.6 (-15.5)</b>
SDM	<b>-48.7 (-9.0)</b>	-17.6 (-6.0)	<b>-147.2 (-27.0)</b>	<b>-61.7 (-20.9)</b>
<i>Extreme precipitation (mm)</i>				
Ref.	31.77	30.53	31.77	30.53
DC	<b>-1.43 (-4.5)</b>	0.40 (1.3)	<b>-6.73 (-21.2)</b>	<b>-3.31 (-10.8)</b>
QM	<b>4.05 (12.7)</b>	<b>6.56 (21.5)</b>	<b>4.10 (12.9)</b>	<b>8.10 (26.5)</b>
SDM	0.48 (1.5)	1.92 (6.3)	0.36 (1.1)	3.86 (12.7)
<i>Average temperature (<math>^{\circ}</math>C)</i>				
Ref.	13.24	14.73	13.24	14.73
DC	<b>1.57</b>	<b>1.47</b>	<b>4.44</b>	<b>4.12</b>
QM	<b>1.43</b>	<b>1.32</b>	<b>4.08</b>	<b>3.81</b>
SDM	<b>1.56</b>	<b>1.40</b>	<b>4.43</b>	<b>4.05</b>

Note: Values marked in bold are significantly different from zero ( $p < 0.05$ ).

project a decrease in the Sierra de Segura catchment (n.s.) and a significant increase in the Guadalentin catchment.

Only five of the 12 scenarios show significant changes in soil loss (Figure 6). Even in those five scenarios the output from the nine climate models (GCM/RCM combinations) is not consistent in the direction of change. For instance, based on the ensemble prediction of nine RCMs the DC method in the far-future scenario projects a significant decrease in soil loss for the Sierra de Segura catchment, whereas the RCA/EC-EARTH climate model ( $\Delta$ ) projects an increase in soil loss for the same period. Some climate models consistently show the opposite change compared to the ensemble average. For instance, in the foreseeable-future scenario the RCA/MPI-ESM-LR climate model ( $\triangledown$ ) projects a decrease in soil loss for all bias correction methods and for both catchments. Nevertheless, in the far-future scenario, this climate

model projects a change often similar to the median of the nine climate models.

## Discussion

Our results show that bias correction methods have a significant influence on the soil loss projections in a temperate and semi-arid catchment. In some scenarios, all three bias correction methods show the same direction of change, i.e. an increase in soil loss in the foreseeable future scenario in the Guadalentin catchment and a decrease in soil loss in the far future scenario in the Sierra de Segura catchment (Figure 6 and Table V). However, the DC method projects the opposite response relative to the QM and SDM methods for the foreseeable-future scenario in the Sierra de Segura catchment and the far-future scenario in the Guadalentin catchment. These differences are mostly related to the changes in the projected extreme precipitation (Figure 4), where a change in extreme precipitation often leads to a similar direction of change in soil loss. For instance, the DC method projects a decrease in extreme precipitation in the Sierra de Segura catchment for the foreseeable-future scenario and in the Guadalentin catchment for both scenarios, corresponding to a decrease in soil loss.

An increase in extreme precipitation does not always result in an increased soil loss. For instance, in the Sierra de Segura catchment in the far-future scenario an increase in extreme precipitation is projected with the QM method, whereas soil loss is projected to decrease. This is mainly caused by a substantial decrease in annual precipitation sum, which is most likely the effect of a decrease in precipitation frequency. Hence, under these circumstances, the number of rain days decreases, which has a more dominant effect on soil loss than changes in extreme precipitation. Another possibility is that land use attenuates the relation between extreme precipitation and soil loss in the Sierra de Segura catchment, which is dominated by natural vegetation (Table I) and may be less sensitive to extreme precipitation. Conversely, in the Guadalentin catchment, which is dominated by agricultural land uses (Table I), even a non-significant increase in extreme precipitation with the SDM method leads to significant increases in soil loss in both future periods. In theory, differences in the

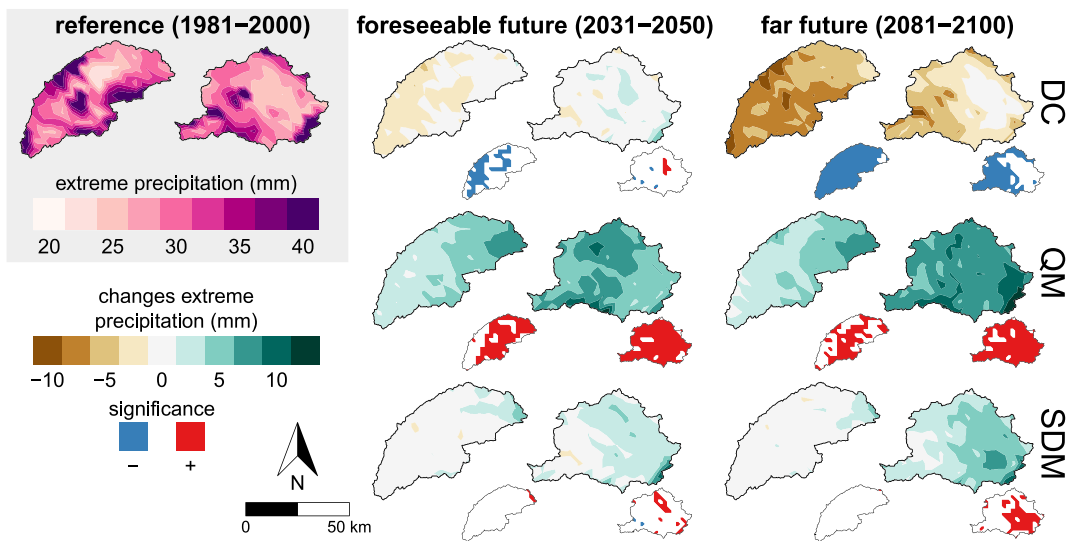


**Figure 4.** Ensemble average heavy precipitation (mm), defined as the 95th percentile of daily precipitation, considering only rainy days ( $>1 \text{ mm d}^{-1}$ ; Jacob *et al.*, 2014), for the reference scenario (1981–2000; left) and changes between the reference scenario and the two future scenarios (2031–2050, middle; 2081–2100, right) for each bias correction method. The small maps in the right bottom corner of each map represent the significance, where blue indicates a significant decrease and red a significant increase ( $p < 0.05$ )

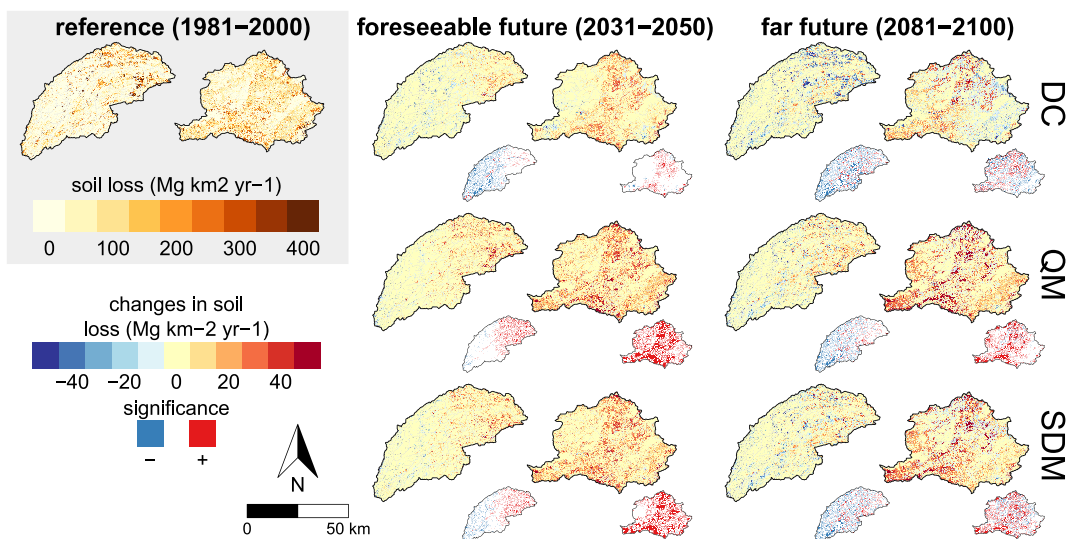


**Figure 5.** Ensemble average annual soil loss ( $\text{Mg km}^{-2} \text{ yr}^{-1}$ ), for the reference scenario (1981–2000; left) and changes between the reference scenario and the two future scenarios (2031–2050, middle; 2081–2100, right) for each bias correction method. The small maps in the right bottom corner of each map represent significance, where blue indicates a significant decrease and red a significant increase ( $p < 0.05$ )

timing of extreme precipitation relative to periods of the year with least vegetation cover may also be different between the bias correction methods, but we did not find such an effect.

To assess the agreement between the bias-corrected projections and the raw climate projections, we quantified how the projected change from the raw climate model output (i.e. change between the raw future and raw historical climate model output) compares to the projected change after bias correction (i.e. change between the bias-corrected future climate projections and observations from the reference period). The results from this analysis indicate that all bias correction methods underestimate the decrease in annual precipitation sum, with the highest projected overestimation with the QM method (Figure 7). The strength and weaknesses of the three bias correction methods are more apparent when relative changes with respect to extreme precipitation are considered. The results clearly show that the DC method underestimates the projected increase in extreme precipitation, although

under certain circumstances the differences with respect to the raw climate signal are relatively small (in the Guadalentin

**Table V.** Catchment-average annual soil loss ( $\text{Mg km}^{-2} \text{ yr}^{-1}$ ) from the reference scenario and difference between the reference and future scenarios and are accompanied with percentages in parentheses

	Foreseeable future (2031–2050)		Far future (2081–2100)	
	Sierra de Segura	Guadalentin	Sierra de Segura	Guadalentin
Ref.	88.6	115.7	88.6	115.7
DC	-3.6 (-4.0)	6.9 (5.9)	<b>-24.4 (-27.5)</b>	-5.0 (-4.3)
QM	11.7 (13.2)	<b>40.6 (35.1)</b>	-6.4 (-7.2)	<b>34.6 (29.9)</b>
SDM	7.5 (8.5)	<b>33.1 (28.6)</b>	-11.9 (-13.4)	<b>23.5 (20.3)</b>

Note: Values marked in bold are significantly different from zero ( $p < 0.05$ ).

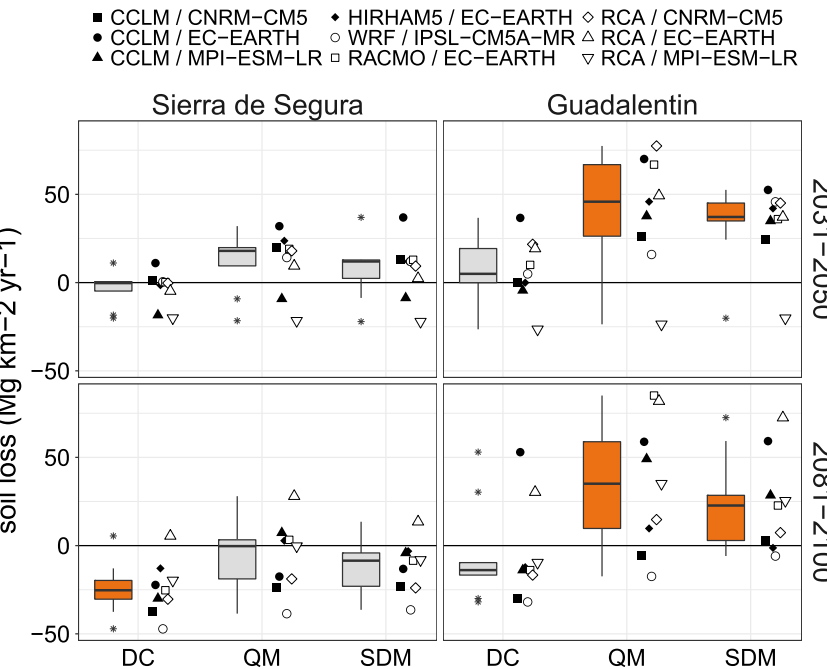


**Figure 6.** Difference of catchment-average annual soil loss ( $\text{Mg km}^{-2} \text{yr}^{-1}$ ) between the reference scenario and future scenarios for each bias correction method. The range of soil loss for each time period, catchment and bias correction method is shown in box plots (left) and individual data points for the nine climate models (GCM/RCM combinations) (right). The orange fill in the box plots indicates a significant change ( $p < 0.05$ )

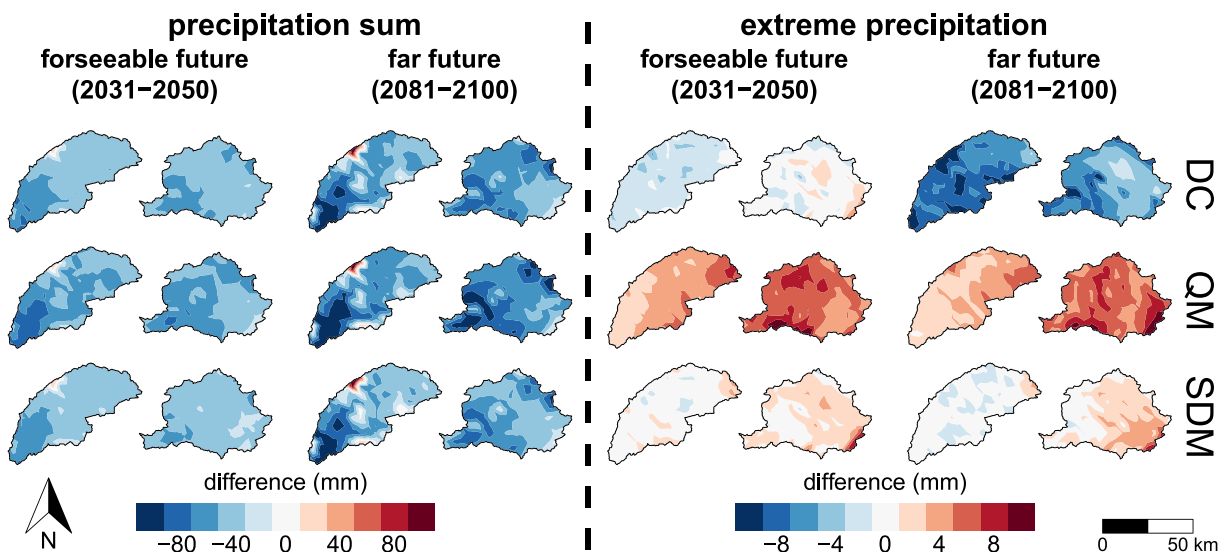


**Figure 7.** Deviation introduced by the three bias correction methods, shown as the difference between the raw and bias-corrected relative precipitation change. A negative value indicates that the bias correction underestimates the climate change signal with respect to the raw climate model projection, and a positive value indicates that the bias correction overestimates the climate signal. Results are shown for precipitation sum (left) and extreme precipitation (right) and for all 12 scenarios

catchment under the foreseeable future scenario). The QM method overestimates the projected increase in extreme precipitation, which is most likely also the cause of the higher overestimation of precipitation sum. The SDM method slightly overestimates the projected increase in extreme precipitation in the Guadalentin catchment, whereas the difference for the Sierra de Segura catchment is close to zero. Hence the SDM method performs best in translating the projected raw climate change signal.

Our results confirm the findings from Mullan *et al.* (2012), who argued that the bias correction methods that provide changes in both the climate mean and variance are most appropriate for soil erosion modelling. The most used method in soil erosion climate change assessments is the DC method

(supporting information, Figure S1), which does not explicitly account for the changes in precipitation distribution and would, therefore, not fit this proposition. Most often, the DC method leads to a similar direction of change for precipitation sum and extreme precipitation. Under some circumstances, the DC method may lead to an opposite direction of change between precipitation sum and extreme precipitation and consequently also of soil erosion – for instance, when an increase in precipitation is projected in a month with a relatively high precipitation sum in the reference period and a decrease is projected in the rest of the year. Nevertheless, by not explicitly accounting for changes in the precipitation distribution, the DC may not be suitable for most soil erosion assessments. Some studies who applied this method have acknowledged

this (e.g. Mukundan *et al.*, 2013; Plangoen *et al.*, 2013), while others also altered the number of rainy days in combination with the DC method (Rodríguez-Blanco *et al.*, 2016) or applied a weather generator in addition to the DC method (e.g. Pruski and Nearing, 2002a; Zhang and Nearing, 2005; Zhang *et al.*, 2012; Hoomehr *et al.*, 2016) to overcome this limitation. A frequently used alternative to the DC method is the QM method, which explicitly accounts for changes in the precipitation distribution. Nevertheless, this method has the limitation that it may overestimate the climate change signal (Maurer and Pierce, 2014), both regarding precipitation intensity and annual volume, as shown by Figure 7. Therefore, we suggest using novel methods that have been shown to outperform the QM method, such as scaled distribution mapping (Switanek *et al.*, 2017).

Here we assessed the impact of climate change on soil erosion with an ensemble of nine climate models (GCM/RCM combinations; see Table II). Climate model output is one of the most dominant sources of uncertainty within climate change impact assessments (Chen *et al.*, 2011b). We showed that even when a scenario was classified as significantly different from the reference scenario individual climate models may project an opposite change in soil loss (Figure 6). We applied a coupled hydrology–soil erosion model, which also reports hydrological variables, such as evapotranspiration, soil moisture and runoff. We determined the coefficient of variation (standard deviation divided by the mean) of these output variables to determine which variables are most sensitive to variation among the climate models. Runoff is the most sensitive model variable, followed by soil loss (Figure 8). Hence, to reduce uncertainty in model projections, climate change impact assessments that focus on model output variables that are sensitive to changes in climate forcing should be assessed with ensemble climate model projections consisting of a larger number of climate models. This will help to both increase the variation of possible future projections and enable us to determine ensemble statistics, such as significance and robustness of the projected model output. The vast majority of the soil erosion climate change assessments only use one climate model (supporting information, Figure S2), which notably limits the statistical significance of the results.

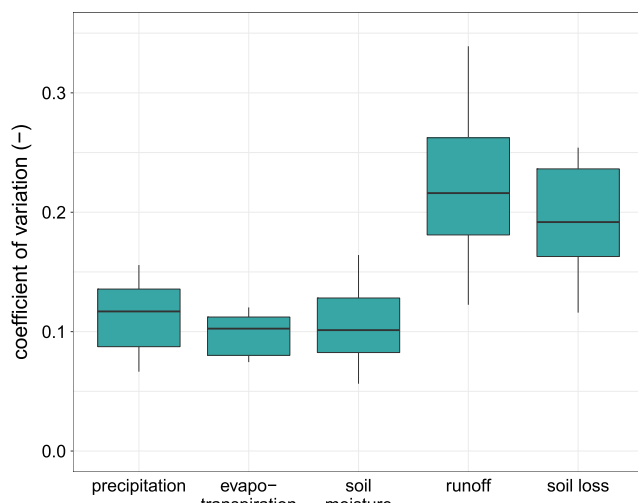


**Figure 8.** Coefficient of variation of hydrological and soil erosion model variables

## Conclusions

The selection of bias correction methods significantly affects the response of future projections in soil loss. Here we applied three bias correction methods in two catchments where climate change is projected to lead to a decrease in annual precipitation, but to an increase in extreme precipitation. We showed that the DC method generally projects a decrease in extreme precipitation, similar to the decrease in annual precipitation, resulting in a decrease in soil loss in most scenarios. While the QM method explicitly accounts for changes in the precipitation distribution, here we show that this method overestimates extreme precipitation, which may lead to an overestimation of the projected soil loss. The third method (SDM) shows the smallest deviation from the raw climate projections. This method allows us to most accurately reproduce the projected extreme precipitation increase, ultimately leading to an increase in soil loss in most scenarios.

Often climate model ensemble projections are used to reduce uncertainty of impact assessments. We included an ensemble of nine climate models (GCM/RCM combinations), to account for differences in projected changes in the climate variables. We determined the significance within the climate model ensemble. Even when projected changes in soil loss were classified as significant, individual climate models projected a change opposite to the ensemble average. Furthermore, soil loss and runoff are among the model output variables with the highest sensitivity, when considering the variation among the output from individual climate models. These findings indicate that climate model ensemble predictions consisting of sufficient climate models are needed to assess the impact of climate change on soil erosion.

The projected climate change signal in the two study catchments shows contrasting projected changes in annual precipitation and extreme precipitation, due to a projected change in the precipitation distribution. Under these circumstances, the impact of climate change on soil erosion can only be assessed when the climate model output is bias corrected with a method that accounts for changes in the precipitation distribution. Following Pierce *et al.* (2015), we suggest first establishing the projected climate change signal from the raw climate model output. Based on this analysis, an appropriate bias correction method can be selected that best reproduces the projected climate change signal. The impact of climate change on soil erosion can only accurately be assessed with a bias correction method that best reproduces the projected climate change signal, in combination with a climate model ensemble.

**Acknowledgements**— We acknowledge financial support from the ‘Juan de la Cierva - Formación’ program of the Spanish Ministerio de Economía y Competitividad (FJCI-2016-28905), the Spanish Ministerio de Economía y Competitividad (ADAPT project; CGL2013-42009-R) and the Séneca foundation of the regional government of Murcia (CAMBIO project; 118933/JLI/13). The authors thank AEMET and UC for the data provided for this work (Spain02 v5 dataset, available at <http://www.meteo.unican.es/datasets/spain02>). We thank the Associate Editor and two anonymous reviewers for their constructive comments on the manuscript.

## References

- Akima H. 1996. Algorithm 761; Scattered-data surface fitting that has the accuracy of a cubic polynomial. *ACM Transactions on Mathematical Software* **22**(3): 362–371. <https://doi.org/10.1145/232826.232856>.
- Blöschl G, Gaál L, Hall J, Kiss A, Komma J, Nester T, Parajka J, Perdigão RAP, Plavcová L, Rogger M, Salinas J L, Viglione A. 2015.

- Increasing river floods: fiction or reality? *Wiley Interdisciplinary Reviews: Water* **2**(4): 329–344. <https://doi.org/10.1002/wat2.1079>.
- Boardman J, Evans R, Favis-Mortlock DT, Harris TM. 1990. Climate change and soil erosion on agricultural land in England and Wales. *Land Degradation and Development* **2**(2): 95–106. <https://doi.org/10.1002/lde.3400020204>.
- Boardman J, Favis-Mortlock DT. 1993. Climate change and soil erosion in Britain. *Geographical Journal* **159**(2): 179–183. <https://doi.org/10.2307/3451408>.
- Boé J, Terray L, Habets F, Martin E. 2007. Statistical and dynamical downscaling of the Seine basin climate for hydro-meteorological studies. *International Journal of Climatology* **27**(12): 1643–1655. <https://doi.org/10.1002/joc.1602>.
- Cannon AJ, Sobie SR, Murdock TQ. 2015. Bias correction of GCM precipitation by quantile mapping: how well do methods preserve changes in quantiles and extremes? *Journal of Climate* **28**(17): 6938–6959. <https://doi.org/10.1175/JCLI-D-14-00754.1>.
- Chen J, Brissette FP, Leconte R. 2011a. Uncertainty of downscaling method in quantifying the impact of climate change on hydrology. *Journal of Hydrology* **401**(3–4): 190–202. <https://doi.org/10.1016/j.jhydrol.2011.02.020>.
- Chen J, Brissette FP, Lucas-Picher P, Caya D. 2017. Impacts of weighting climate models for hydro-meteorological climate change studies. *Journal of Hydrology* **549**: 534–546. <https://doi.org/10.1016/j.jhydrol.2017.04.025>.
- Chen J, Brissette FP, Poulin A, Leconte R. 2011b. Overall uncertainty study of the hydrological impacts of climate change for a Canadian watershed. *Water Resources Research* **47**(12): 1–16. <https://doi.org/10.1029/2011WR010602>.
- Correa SW, Mello CR, Chou SC, Curi N, Norton LD. 2016. Soil erosion risk associated with climate change at Mantaro River basin, Peruvian Andes. *CATENA* **147**: 110–124. <https://doi.org/10.1016/j.catena.2016.07.003>.
- Crozier M. 2010. Deciphering the effect of climate change on landslide activity: a review. *Geomorphology* **124**(3–4): 260–267. <https://doi.org/10.1016/j.geomorph.2010.04.009>.
- Déqué M. 2007. Frequency of precipitation and temperature extremes over France in an anthropogenic scenario: Model results and statistical correction according to observed values. *Global and Planetary Change* **57**(1–2): 16–26. <https://doi.org/10.1016/j.gloplacha.2006.11.030>.
- Eekhout JPC, Hunink JE, Terink W, de Vente J. 2018a. Why increased extreme precipitation under climate change negatively affects water security. *Hydrology and Earth System Sciences* **22**(11): 5935–5946. <https://doi.org/10.5194/hess-2018-161>.
- Eekhout JPC, Terink W, de Vente J. 2018b. Assessing the large-scale impacts of environmental change using a coupled hydrology and soil erosion model. *Earth Surface Dynamics* **6**(3): 687–703. <https://doi.org/10.5194/esurf-6-687-2018>.
- Farr TG, Rosen PA, Caro E, Crippen R, Duren R, Hensley S. 2007. The shuttle radar topography mission. *Reviews of Geophysics* **45**(2): RG2004. <https://doi.org/10.1029/2005RG000183>.
- Favis-Mortlock D, Evans R, Boardman J, Harris T. 1991. Climate change, winter wheat yield and soil erosion on the English south downs. *Agricultural Systems* **37**(4): 415–433. [https://doi.org/10.1016/0308-521X\(91\)90062-F](https://doi.org/10.1016/0308-521X(91)90062-F).
- Giorgi F, Jones C, Asrar GR. 2009. Addressing climate information needs at the regional level: The CORDEX framework. *World Meteorological Organization Bulletin* **58**(3): 175–183.
- Hempel S, Frieler K, Warszawski L, Schewe J, Piontek F. 2013. A trend-preserving bias correction: The ISI-MIP approach. *Earth System Dynamics* **4**(2): 219–236. <https://doi.org/10.5194/esd-4-219-2013>.
- Hengl T, de Jesus JM, Heuvelink GBM, Ruiperez Gonzalez M, Kilibarda M, Blagotic A, et al. 2017. Soilgrids250m: Global gridded soil information based on machine learning. *PLOS ONE* **12**(2): e0169748. <https://doi.org/10.1371/journal.pone.0169748>.
- Herrera S, Fernández J, Gutiérrez JM. 2016. Update of the Spain02 gridded observational dataset for EURO-CORDEX evaluation: Assessing the effect of the interpolation methodology. *International Journal of Climatology* **36**(2): 900–908. <https://doi.org/10.1002/joc.4391>.
- Hertig E, Paxian A, Vogt G, Seubert S, Paeth H, Jacobbeit J. 2012. Statistical and dynamical downscaling assessments of precipitation extremes in the Mediterranean area. *Meteorologische Zeitschrift* **21**(1): 61–77. <https://doi.org/10.1127/0941-2948/2012/0271>.
- Hoomehr S, Schwartz JS, Yoder DC. 2016. Potential changes in rainfall erosivity under GCM climate change scenarios for the southern Appalachian region, USA. *CATENA* **136**: 141–151. <https://doi.org/10.1016/j.catena.2015.01.012>.
- Houska T, Kraft P, Chamorro-Chavez A, Breuer L. 2015. SPOTTing model parameters using a ready-made python package. *PLOS ONE* **10**(12): 1–22. <https://doi.org/10.1371/journal.pone.0145180>.
- Jacob D, Petersen J, Eggert B, Alias A, Christensen OB, Bouwer LM, Braun A, Colette A, Déqué M, Georgievski G, Georgopoulou E, Gobiet A, Menut L, Nikulin G, Haensler A, Hempelmann N, Jones C, Keuler K, Kovats S, Kröner N. 2014. EURO-CORDEX: New high-resolution climate change projections for European impact research. *Regional Environmental Change* **14**(2): 563–578. <https://doi.org/10.1007/s10113-013-0499-2>.
- Kourgialas NN, Koubouris GC, Karatzas GP, Metzidakis I. 2016. Assessing water erosion in Mediterranean tree crops using GIS techniques and field measurements: The effect of climate change. *Natural Hazards* **83**(S1): 65–81. <https://doi.org/10.1007/s11069-016-2354-5>.
- Lacoste M, Viaud V, Michot D, Walter C. 2015. Landscape-scale modelling of erosion processes and soil carbon dynamics under land-use and climate change in agroecosystems. *European Journal of Soil Science* **66**(4): 780–791. <https://doi.org/10.1111/ejss.12267>.
- Ladson AR, Brown R, Neal B, Nathan R. 2013. A standard approach to baseflow separation using the Lyne and Hollick filter. *Australasian Journal of Water Resources* **17**(1): 25–34.
- Le Roux R, Katurji M, Zawar-Reza P, Quénol H, Sturman A. 2018. Comparison of statistical and dynamical downscaling results from the WRF model. *Environmental Modelling and Software* **100**: 67–73. <https://doi.org/10.1016/j.envsoft.2017.11.002>.
- Li Z, Fang H. 2016. Impacts of climate change on water erosion: A review. *Earth-Science Reviews* **163**: 94–117. <https://doi.org/10.1016/j.earscirev.2016.10.004>.
- MAPAMA. 2010. Mapa de Cultivos y Aprovechamientos de España 2000–2010 (1:50.000).
- Maetens W, Vanmaercke M, Poesen J, Jankauskas B, Jankauskiene G, Ionita I. 2012. Effects of land use on annual runoff and soil loss in Europe and the Mediterranean: A meta-analysis of plot data. *Progress in Physical Geography* **36**(5): 599–653. <https://doi.org/10.1177/030913312451303>.
- Maraun D, Wetterhall F, Ireson AM, Chandler RE, Kendon EJ, Widmann M, Brieren S, Rust HW, Sauter T, Themessl M, Venema VKC, Chun KP, Goodess CM, Jones RG, Onof C, Vrac M, Thiele-Eich I. 2010. Precipitation downscaling under climate change: Recent developments to bridge the gap between dynamical models and the end user. *Reviews of Geophysics* **48**(3): RG3003. <https://doi.org/10.1029/2009RG000314>.
- Maurer EP, Pierce DW. 2014. Bias correction can modify climate model simulated precipitation changes without adverse effect on the ensemble mean. *Hydrology and Earth System Sciences* **18**(3): 915–925. <https://doi.org/10.5194/hess-18-915-2014>.
- Morgan RPC, Duzant JH. 2008. Modified MMF (Morgan–Morgan–Finney) model for evaluating effects of crops and vegetation cover on soil erosion. *Earth Surface Processes and Landforms* **33**(1): 90–106. <https://doi.org/10.1002/esp.1530>.
- Mukundan R, Pradhanang SM, Schneiderman EM, Pierson DC, Anandhi A, Zion MS, Matonse AH, Lounsbury DG, Steenhuis TS. 2013. Suspended sediment source areas and future climate impact on soil erosion and sediment yield in a New York City water supply watershed, USA. *Geomorphology* **183**(June): 110–119. <https://doi.org/10.1016/j.geomorph.2012.06.021>.
- Mullan D, Favis-Mortlock D, Fealy R. 2012. Addressing key limitations associated with modelling soil erosion under the impacts of future climate change. *Agricultural and Forest Meteorology* **156**(June 2016): 18–30. <https://doi.org/10.1016/j.agrformet.2011.12.004>.
- Nash JE, Sutcliffe JV. 1970. River flow forecasting through conceptual models. Part I: A Discussion of principles. *Journal of Hydrology* **10**: 282–290. [https://doi.org/10.1016/0022-1694\(70\)90255-6](https://doi.org/10.1016/0022-1694(70)90255-6).
- Nearing M, Deer-Ascough L, Lafren JM. 1990. Sensitivity analysis of the Wepp hillslope profile erosion model. *Transactions of the ASAE* **33**(3): 0839–0849. <https://doi.org/10.13031/2013.31409>.

- Nearing MA, Pruski FF, O'Neal MR. 2004. Expected climate change impacts on soil erosion rates: A review. *Journal of Soil and Water Conservation* **59**(1): 43–50.
- Nunes JP, Seixas J, Keizer JJ, Ferreira AJD. 2009. Sensitivity of runoff and soil erosion to climate change in two Mediterranean watersheds. Part II: Assessing impacts from changes in storm rainfall, soil moisture and vegetation cover. *Hydrological Processes* **23**(8): 1212–1220. <https://doi.org/10.1002/hyp.7250>.
- Paroissien J-B, Darboux F, Couturier A, Devillers B, Mouillot F, Raclot D, Le Bissonnais Y. 2015. A method for modeling the effects of climate and land use changes on erosion and sustainability of soil in a Mediterranean watershed (Languedoc, France). *Journal of Environmental Management* **150**: 57–68. <https://doi.org/10.1016/j.jenvman.2014.10.034>, 2015.
- Pierce DW, Cayan DR, Maurer EP, Abatzoglou JT, Hegewisch KC. 2015. Improved bias correction techniques for hydrological simulations of climate change. *Journal of Hydrometeorology* **16**(6): 2421–2442. <https://doi.org/10.1175/JHM-D-14-0236.1>.
- Plangoen P, Babel M, Clemente R, Shrestha S, Tripathi N. 2013. Simulating the impact of future land use and climate change on soil erosion and deposition in the Mae Nam Nan Sub-Catchment, Thailand. *Sustainability* **5**(8): 3244–3274. <https://doi.org/10.3390/su5083244>.
- Pruski FF, Nearing MA. 2002a. Climate-induced changes in erosion during the 21st century for eight U.S.locations. *Water Resources Research* **38**(12): 34–1–34–11. <https://doi.org/10.1029/2001WR000493>.
- Pruski FF, Nearing MA. 2002b. Runoff and soil loss responses to changes in precipitation: A computer simulation study. *Journal of Soil and Water Conservation* **57**(1): 7–16.
- Rodríguez-Blanco M, Arias R, Taboada-Castro M, Nunes J, Keizer J, Taboada-Castro M. 2016. Potential impact of climate change on suspended sediment yield in NW Spain: A case study on the Corbeira Catchment. *Water* **8**(12): 444. <https://doi.org/10.3390/w8100444>.
- Routschek A, Schmidt J, Enke W, Deutschlaender T. 2014. Future soil erosion risk: Results of GIS-based model simulations for a catchment in Saxony/Germany. *Geomorphology* **206**: 299–306. <https://doi.org/10.1016/j.geomorph.2013.09.033>.
- Serrano-Notivoli R, Beguería S, Saz MÁ, Longares LA, de Luis M. 2017. SPREAD: A high-resolution daily gridded precipitation dataset for Spain – an extreme events frequency and intensity overview. *Earth System Science Data* **9**(2): 721–738. <https://doi.org/10.5194/essd-9-721-2017>.
- Shrestha B, Babel MS, Maskey S, van Griensven A, Uhlenbrook S, Green A, Akkharath I. 2013. Impact of climate change on sediment yield in the Mekong River basin: A case study of the Nam Ou basin, Lao PDR. *Hydrology and Earth System Sciences* **17**(1): 1–20. <https://doi.org/10.5194/hess-17-1-2013>.
- Sun Y, Solomon S, Dai A, Portmann RW. 2007. How often will it rain? *Journal of Climate* **20**(19): 4801–4818. <https://doi.org/10.1175/JCLI4263.1>.
- Switanek BM, Troch AP, Castro LC, Leuprecht A, Chang HI, Mukherjee R, Demaria MC. 2017. Scaled distribution mapping: A bias correction method that preserves raw climate model projected changes. *Hydrology and Earth System Sciences* **21**(6): 2649–2666. <https://doi.org/10.5194/hess-21-2649-2017>.
- Terink W, Lutz AF, Simons GWH, Immerzeel WW, Droogers P. 2015. SPHY V2.0: Spatial Processes in HYdrology. *Geoscientific Model Development* **8**(7): 2009–2034. <https://doi.org/10.5194/gmd-8-2009-2015>.
- Teutschbein C, Seibert J. 2010. Regional climate models for hydrological impact studies at the catchment scale: A review of recent modeling strategies. *Geography Compass* **4**(7): 834–860. <https://doi.org/10.1111/j.1749-8198.2010.00357.x>.
- Teutschbein C, Seibert J. 2012. Bias correction of regional climate model simulations for hydrological climate-change impact studies: Review and evaluation of different methods. *Journal of Hydrology* **456–457**: 12–29. <https://doi.org/10.1016/j.jhydrol.2012.05.052>.
- Themeßl MJ, Gobiet A, Heinrich G. 2012. Empirical-statistical downscaling and error correction of regional climate models and its impact on the climate change signal. *Climatic Change* **112**(2): 449–468. <https://doi.org/10.1007/s10584-011-0224-4>.
- Vaittinada Ayar P, Vrac M, Bastin S, Carreau J, Déqué M, Gallardo C. 2016. Intercomparison of statistical and dynamical downscaling models under the EURO- and MED-CORDEX initiative framework: Present climate evaluations. *Climate Dynamics* **46**(3–4): 1301–1329. <https://doi.org/10.1007/s00382-015-2647-5>.
- Wood AW, Leung LR, Sridhar V, Lettenmaier DP. 2004. Hydrologic implications of dynamical and statistical approaches to downscaling climate model outputs. *Climatic Change* **62**(1–3): 189–216. <https://doi.org/10.1023/B:CLIM.0000013685.99609.9e>.
- Zhang Y, Hernandez M, Anson E, Nearing MA, Wei H, Stone JJ, Heilman P. 2012. Modeling climate change effects on runoff and soil erosion in southeastern Arizona rangelands and implications for mitigation with conservation practices. *Journal of Soil and Water Conservation* **67**(5): 390–405. <https://doi.org/10.2489/jswc.67.5.390>.
- Zhang XC, Nearing MA. 2005. Impact of climate change on soil erosion, runoff, and wheat productivity in central Oklahoma. *CATENA* **61**(2–3): 185–195. <https://doi.org/10.1016/j.catena.2005.03.009>.

## Supporting Information

Supporting information may be found in the online version of this article.